HHS Public Access

Author manuscript

J Neural Eng. Author manuscript; available in PMC 2019 December 01.

Published in final edited form as:

J Neural Eng. 2018 December ; 15(6): 064001. doi:10.1088/1741-2552/aae129.

Methods for Fabrication and Evaluation of a 3D Microengineered Model of Myelinated Peripheral Nerve

Parastoo Khoshakhlagh[#1], **Ashwin Sivakumar**[#1], **Lauren A Pace**[2], **Daniel W Sazer**[1], and **Michael J Moore**[1,2,3,*]

[1]Department of Biomedical Engineering, Tulane University, New Orleans, 70118, LA, USA

[2]AxoSim Technologies, New Orleans, 70112, LA, USA

[3]Tulane Brain Institute, Tulane University, New Orleans, 70118, LA, USA

[#] These authors contributed equally to this work.

Abstract

Objective.—The cost and low success rates of the neurological drug development pipeline have diverted the pharmaceutical industry to 'nerve-on-a-chip' systems as preclinical models to streamline drug development. We present a novel micro-engineered 3D hydrogel platform for the culture of myelinated embryonic peripheral neural tissue to serve as an effective *in vitro* model for electrophysiological and histological analysis that could be adopted for preclinical testing.

Approach.—Dorsal root ganglions (DRG) from 15-day old embryonic rats were cultured in 3D hydrogel platforms. The interaction between Schwann cells (SC) and neurons during axonal development and regeneration affects the direction of growth and the synthesis of myelin sheaths. Induction of myelination was performed with two approaches: the addition of exogenous SC and promoting migration of endogenous SC.

Main results.—Histological analysis of the preparation utilizing exogenous SC showed aligned, highly fasciculated axonal growth with noticeable myelin sheaths around axons. Separately, electrophysiological testing of the preparation utilizing endogenous SC showed increased amplitude of the compound action potential and nerve conduction velocity in the presence of ascorbic acid (AA)

Significance.—This platform has immense potential to be a useful and translatable *in vitro* testing tool for drug discovery and myelination studies.

[*]Corresponding author: mooremj@tulane.edu. Author contributions statement.

AS and PK conceived and performed experiments, analyzed results, and wrote sections of the manuscript. LAP performed experiments, analyzed results, and contributed writing. DWS performed experiments and analyzed results. MJM conceived experiments and wrote sections of the manuscript. All authors reviewed all portions of the manuscript.

Competing Financial Interests

PK and MJM are inventors on a patent that has been filed and is pending at the time of submission of this article. MJM is a co-founder, officer, and equity stakeholder in a startup company that has licensed the myelinated nerve-on-chip technology described. LAP is a paid employee of the company at the time of writing this article.

Data availability

The data that support the findings of this study and the protocols utilized are available from the corresponding author on request.

1. Introduction

Plagued with skyrocketing costs and low success rates of the drug development pipeline, the pharmaceutical industry is increasingly turning toward microphysiological systems, or "organs-on-chips", as preclinical models for drug development[1,2]. This approach could be particularly beneficial for neurological applications, where the failure rate of drugs entering Phase I clinical trials is as high as 92%[3]. Such high attrition rates have motivated accelerated development of neural microphysiological systems in recent years[4,5]. Modeling the nervous system is challenging compared to other organ systems due to its complex architecture, the need for electrophysiological measurements, and the relative difficulty of culturing neural cells. In particular, models of the peripheral nervous system (PNS) have not been developed with suitable urgency. While peripheral nerve disorders are rarely life-threatening, drug-induced neuropathy is a major cause of experimental drug failure[6]. The need for preclinical models that can recapitulate certain key physiological aspects of the nervous system remains acute.

Microphysiological systems that seek to recapitulate the most relevant physiological phenomena in a simple model require a strong focus on system architecture[7,8]. Myelin is a critical feature within the nervous system that should be considered in on-a-chip applications. In addition to contributing to fast, saltatory axonal conduction, myelinating Schwann cells (SC) play major roles in peripheral neuronal axon growth, homeostasis, and regeneration[9]. Co-cultures of neurons and SC have provided insights into biological mechanisms of SC-neuron interactions in numerous studies[10–12]. However, typical co-cultures do not reflect the architecture and dimensionality of peripheral nerve tissue. This may be important for certain applications, because neural cultures prepared in certain 3D configurations have been shown to more closely reflect *in vivo* neurophysiology. For example, it has been shown that resting potential, action potential propagation, the function of voltage-gated channels, and network dynamics are significantly altered in 2D configurations, compared to 3D configurations and intact tissue[13–17]. Thus, a 3D culture configuration is expected to be important for preclinical models that incorporate myelination.

We propose that there remains a need for high-content phenotypic assays whose metrics may be readily compared with *in vivo* animal or clinical data. Nerve conduction testing and histopathology have been used for decades in both preclinical animal and clinical human settings to assess peripheral nerve health for toxicology and neurodegenerative disorders[18–21]. In contrast, multiwell, *in vitro* assays of neurite outgrowth and microelectrode array electrophysiology have emerged as potentially high-throughput models of peripheral nerve biology useful for screening large numbers of compounds[22–24]. Neurons assayed in these manners are typically unmyelinated, and it may be challenging to translate findings to clinical outcomes. Thus, a preclinical model of a myelinated peripheral nerve that enables evaluation of both nerve conduction and histopathology would represent an important contribution.

Our objective was to expand on our prior nerve-on-a-chip formed in dual micropatterned hydrogels[25] to develop a physiologically relevant model of myelinated peripheral nerve that

enabled evaluation with nerve conduction and histology. However, this objective was challenged by a number of conflicting design constraints, including hydrogel stability, cell viability, transparency, and ease of histology. Self-assembling hydrogels were susceptible to detaching from PEG hydrogel molds[26] while photocrosslinking was found to be disproportionately harmful to Schwann cells[27]. Preliminary work with alternative hydrogels showed that methacrylated dextran cured with visible light and a riboflavin-arginine photoinitiator was less phototoxic to Schwann cells, but its yellowish translucent color made it difficult to visualize the tissue for placement of extracellular field electrodes. Conversely, methacrylated heparin facilitated extracellular field recording, but was not compatible with the visible light photoinitiator and was not amenable to resin or paraffin embedding for histology.

In this note, we share progress toward developing a physiologically relevant model of peripheral nerve that may be evaluated with both nerve conduction and histology. We overcame the design constraints by implementing two parallel versions of the model, both utilizing dorsal root ganglion (DRG) explants cultured in 3D hydrogels. In one iteration of the model, DRGs and additional Schwann cells were encapsulated in a visible-light cured, methacrylated dextran (MeDex) gel. This model was used primarily for evaluation with immunohistochemistry and histology. In the second iteration, DRGs were inserted into a cured methacrylated heparin (MeHp) hydrogel and Schwann cells endogenous to the explant were stimulated to form myelin. This version of the model was evaluated with electrophysiology.

Taken together, these complementary in vitro systems allow collection of clinically-relevant endpoints in a model possessing the appropriate 3D architecture and physiology of myelinated peripheral nerve. They provide a unique platform that will be further developed as a preclinical model for studying demyelinating disorders or to assess the safety and efficacy of drugs and their interactions with peripheral nerve.

2. Methods

2.1. Overview

Our goal was to develop a 3D model of myelinated peripheral nerve that could be assessed with histology and nerve conduction measurements. We overcame conflicting design constraints within our system by utilizing two parallel methods, as depicted in Figure 1. For both methods, a dual hydrogel culture environment was used with growth-restrictive polyethylene glycol (PEG) as the boundary hydrogel. Method A used DRGs and additional exogenous SCs encapsulated in growth-permissive methacrylated dextran (MeDex) cured with visible light. This method was compatible mainly with immunohistochemistry and histology. Method B consisted of DRGs, containing endogenous SCs, inserted into growth-promoting methacrylated heparin (MeHp) that was crosslinked with ultraviolet (UV) light prior to insertion of tissue explants. This method, while incompatible with exogenous SCs, facilitated electrophysiological recording.

2.2. Fabrication of Dual Hydrogel System

The dual hydrogel culture system was fabricated using digital projection photolithography, as previously described[25,28–33]. Briefly, the photolithography apparatus was composed of a collimated UV light source (OmniCure 1000 with 320–500 nm filter, EXFO, Quebec, Canada) and visible light source (SOLA light engine with 375–650 nm filter, Lumencor, OR, USA), a digital micromirror device (DMD; Discovery™ 3000, Texas Instruments, Dallas, TX) as a dynamic photomask and a 2X Plan Fluor objective lens (Nikon Instruments, Tokyo, Japan).

This setup was utilized to irradiate a photocurable dual hydrogel system contained within a permeable cell culture insert (Transwell Clear Polyester Membrane Inserts, Corning Inc., Corning, NY, USA) of 0.4μm pore size. Each insert was treated with filtered Rain-X original glass treatment (RainX, Houston, TX) prior to addition of the hydrogel solution to prevent meniscus formation. The dual hydrogel system is comprised of a cell-restrictive component that served as a hydrogel mold and a cell-permissive component in which neurons were cultured. To fabricate the cell-restrictive micro-mold, 0.5mL of a solution of 10% (w/v) PEG-diacrylate (Mn 1000; Polysciences Inc., Warrington, PA) and 0.5% (w/v) Irgacure 2959 in PBS was added to each 6-well plate insert and irradiated with 85 mW/cm^2 UV light as measured by a radiometer (306 UV Powermeter, Optical Associates, San Jose, CA), for 38s (Figure 1). As demonstrated previously, 0.5 mL volume of gel solution yielded a gel of 480 μm thickness[26]. The hydrogel constructs were washed in PBS with 1% antibiotic-antimycotic prior to the addition of cells.

2.3. Synthesis, Characterization, and Composition of Dextran & Heparin Gels

For Method A, dextran (MW = 70 kDa) was grafted with glycidyl methacrylate (GMA) for use in the cell-permissive hydrogel component. Initially, 1 g of dextran was weighed and added to 9 ml dimethylsulfoxide (DMSO) under nitrogen then 0.2 g 4-dimethylaminopyridine (DMAP) was dissolved in 1 ml of DMSO. Subsequently, the DMAP solution was added dropwise to the dextran solution followed by addition of 232 μl GMA under nitrogen. The final solution was stirred for 48 hours (hrs) at room temperature then 280 μl 37% hydrochloric acid (HCl) was then added to the solution to quench the reaction, and this product was dialyzed against deionized water for 3 days and lyophilized for 2 days. This resulted in glycidyl methacrylate-dextran (MeDex), the composition of which was confirmed using ^{1}H NMR [(D_2O) δ 6.1–5.7 (m, 2H, CH_2), δ 5.2 (m, 1H, CH), δ 4.9 (m, 1H, CH), δ 1.9 (s, 3H, CH_3)] with substitution degree of 42%[32,34,35]. Finally, a gel composition of MeDex 50% (w/v), arginine (0.1% (w/w) of MeDex), riboflavin (0.001% (w/w) of MeDex), TEMED (0.2% (v/v) of the final solution) was prepared for photocrosslinking[27].

For Method B, a 4% (w/v) MeHp solution was also created by dissolving heparin sodium salt from porcine intestinal mucosa (Sigma-Aldrich) in PBS and reacting it with glycidyl methacrylate (Aldrich). The MeHp solution was pipetted into the empty voids in the PEG boundary until it was full. The MeHp solution was then irradiated with 85 mW/cm^2 UV light as measured by a radiometer (306 UV Powermeter) for 60 seconds. Following fabrication, the constructs were washed 3 times with a 2% wash solution containing PBS and antibiotic-antimycotic to remove any leftover solution and to improve sterility.

2.4. Primary Tissue Culture in the Dual Hydrogel System

For Method A, the primary culture of rat DRGs was performed as follows. The prepared PEG constructs were immersed in adhesion media containing Neurobasal medium supplemented with B27 (2% v/v), L-glutamine (0.25% v/v), nerve growth factor (NGF) (0.02 μg/ml), fetal bovine serum (FBS) (10% v/v) and penicillin/streptomycin (1% v/v) (Life Technologies, CA, USA) and incubated overnight. Each PEG construct was then cultured with a single Long Evans rat embryonic DRG explant isolated from day 15 embryos according to the guidelines of the Institutional Animal Care and Use Committee. The DRGs were then incubated in fresh adhesion media overnight to allow the tissue to adhere to the insert. For Method B, DRG explants were carefully placed in the hydrogel constructs in the MeHp gel. 2ml of Neural Growth (NG) media containing B27 (2% v/v), L-glutamine (0.25% v/v), NGF (0.02 μg/ml), and Anti-Anti (1% v/v) (Life Technologies, CA, USA) (Table 1) was added underneath the tissue culture inserts overnight to hydrate the gel with media to start neurite growth upon tissue explantation.

2.5. Exogenous Schwann Cell Culture and Encapsulation

SC isolated from neonatal rat sciatic nerves (ScienCell Research Laboratories) were utilized for Method A. The cells were plated on poly-L-lysine-coated culture vessel to encourage cell attachment with a seeding density of ≥ 10,000 cells/cm^2 for 16 hrs. The SC culture medium containing FBS (5% v/v), penicillin/streptomycin (1% v/v) and SC medium supplement (1% v/v) (ScienCell Research Laboratories) was changed after an initial 24 hrs and every 48 hrs thereafter. SC were passaged once they reached 90% confluence and used after the 3rdpassage. SC were dispersed in 50% MeDex solution in SC medium to reach a cell count of 2.0 × 10^7 cell/ml and mixed well to achieve an evenly distributed single cell solution. The adhesion media was then aspirated from the channels gently to avoid disturbing the adhered DRGs, and 2 μl of the MeDex single cell solution was added to each PEG micro-mold. A negative photomask was loaded on the DMD and the gel solution in the channel was crosslinked by 30s irradiations with 85 mW/cm^2 visible light using a SOLA Light Engine with 375–650nm filter (Lumencor) as measured by a radiometer (306 UV Powermeter, Optical Associates). From here, the constructs were gently washed 3x in wash buffer.

2.6. Media Preparations

To achieve the right conditions for myelination, three different types of media were used (Table 1).In method A, exogenous SC preparation, two different media regimens were used. The first regimen comprised two phases in which premyelination and myelination media were consecutively applied for 10 days then 15 days, respectively, based on a previously described method by Eshed et al. which promoted growth, neurite extension and SC myelination of the DRG[36]. The second regimen only applied myelination media for 25 days. In method B, the endogenous SC preparation, a single media regimen comprising of the three different medias were used. NG media was used on the day of DRG explantation followed by 7 days of premyelination media, and then switched over to myelination media. The media were refreshed every other day for all specimens.

2.7. Field Potential Recording

The 3D hydrogel constructs were subject to electrophysiological testing as shown in Figure 2. A concentric bipolar electrode (FHC Inc) was used to deliver a 15 V input on the distal end of the construct, away from the region of DRG implantation while a glass micropipette, filled with artificial cerebrospinal fluid (ACSF), was used to measure the amplitude of the compound action potential (CAP) and peak latency (PL) using LabChart software (AD Instruments). The data files were exported as text files for analysis with a custom MATLAB program. The distance between the recording electrode and stimulating electrode was measured using the Moticam 580 microscope camera and Motic Images Plus (Motic Inc). The PL and the distance measured are also used to determine the nerve conduction velocity (NCV), which shows the speed of the response. The CAP and PL from each construct were averaged from values of 15 consecutive stimulations followed by statistical analyses using the statistical software Prism 7 (GraphPad Software Inc).

2.8. Immunohistochemistry

To evaluate neurite growth and myelin formation, the tissue was fixed with 4% paraformaldehyde (PFA) for 2 hrs at 37° C followed by 3 washing steps prior to each staining procedure. Neurites were labeled with mouse monoclonal [2G10] neuron- specific beta-III tubulin primary antibody and Cy3.5 conjugated goat anti-mouse immunoglobulinG (H + L) secondary antibody. Each labeling step was carried out in PBS containing 2% bovine serum albumin (BSA) and 0.1% saponin, overnight at 4° C followed by 3 washing steps with PBS. To detect myelinating SCs, constructs were labeled for myelin basic protein (MBP) using primary antibody chicken polyclonal anti-Myelin Basic Protein. Constructs were blocked in 5% goat serum for 30 minutes (mins) at room temperature, stored at 4°C overnight in primary antibody solution then washed 3 times with PBS. After three washing cycles the hydrogel systems were incubated at 4° C in a secondary antibody solution that was prepared as follows: 1:500 antibody solution in 2% BSA solution Goat Anti-Chicken IgY H&L. All primary and secondary antibodies were purchased from Abcam.

2.9. Image Processing, Neurite Growth, Myelin Formation

The volume of cell growth into the 3D hydrogel was measured by confocal microscopy (NikonA1). Because of the entangled and dense neurite outgrowth, quantifying the number of individual neurons along the length of neurite extension was difficult. Rather, 3D cell growth was quantified using the volume of cellular mass in the dual hydrogel culture systems. Z-stacks were obtained for each sample with optical slices of a depth no greater than 11 μm, yielding an average of 20 slices per sample at a resolution of 1024 × 1024 pixels using a 10X objective lens.

All images were pre-processed by uniform thresholding, followed by transformation into a binary representation. Data analysis was performed using ImageJ (NIH) and a custom algorithm in MATLAB (Mathworks). Neurite growth was quantified using pixel counts throughout the depth of the gel. In addition, a large image Z-stack (1×5) was taken for each imaging procedure detailed above and maximum intensity projection was then acquired to form 2D images of the total neurite growth.

2.10. Tissue Embedding, Transmission Electron Microscopy (TEM), and Toluidine Blue (TB) Staining

TEM and light microscopy of TB staining were utilized to investigate the nanoscale structure of neuronal processes and SCs, and their spatial crosstalk, distribution, and morphology in the hydrogel cultures. All the reagents used for this procedure were provided from Electron Microscopy Sciences (Hatfield) unless otherwise stated. The hydrogel constructs were fixed after submerging in 4% PFA solution for 2 hrs at 37°C. The samples were then washed three times with PBS at 15 mins intervals. The post-fixation steps included staining with 1% osmium tetroxide (OsO_4) in 100 mM phosphate acetate for 2 hrs followed by 4 washing steps with PBS. The tissue was then stained with 2% aqueous uranyl acetate for 30 mins at room temperature in the dark, then dehydrated by immersion in 50% and 70% ethanol for 10 mins, then 95% ethanol overnight. The samples were then soaked in 100% ethanol that was filtered with Molecular Sieves, 4A (Sigma-Aldrich) for two 30 mins intervals. After this step, the constructs were cut to only maintain the regions of interest. Next, an infiltration step was performed using a 1:1 propylene oxide-spurr resin for 45 mins. The samples were then embedded in 100% spurr resin at 70°C for 48 hrs to allow the resin polymerization to complete. Embedded samples were trimmed and sliced with thicknesses of 80 nm and 500 nm using a Reichert Ultracut S ultratome (Leica Microsystems) and Ultra 45° diamond knife (Diatome).

For TEM, the 80 nm slices were loaded on copper grids (Formvar carbon-coated, 200 mesh) and floated on droplets of 2% uranyl acetate for 20 mins, then rinsed by floating on deionized (DI) water droplets 3 times, for 1 min. After mounting the grids on a single tilted stage, they were imaged using a Tecnai G2 F30 Twin (FEI) with an accelerator voltage of 100–200 kV. Images were taken at 3,000–20,000x magnifications with 4000 × 4000-pixel resolution. The 500 nm slices were floated on droplets of DI water, allowed to dry on glass slides, then stained with a 1% TB acid solution for 30 seconds. 100xLM images were collected using a Nikon Eclipse Ti2 inverted microscope (Nikon Instruments).

2.11. Statistical Analysis

Statistical analysis of significance was done using a two-way ANOVA and Sidak's multiple comparison test post-hoc with equal variance at a $p < 0.05$ for all experiments.

3. Results

The 3D microfabrication method used in this work presents the opportunity to either exogenously incorporate or endogenously promote SCs for 3D myelin formation (Figure 1). The robustness of the system used in this experiment was established using two separate proof-of-concept demonstrations through the utilization of two characteristically different hydrogels. In Method A utilizing exogenous SC, MeDex hydrogel was used as the growth matrix. This model offered spatiotemporally controlled incorporation of exogenous SC by visible light photocrosslinking encapsulation with myelin sheaths observed around axons in histological sections. In Method B, a MeHp hydrogel was utilized and the endogenous SC were encouraged to migrate from DRG explants and form myelin sheaths in a directed manner. The transparent nature of the MeHp hydrogel facilitated the placement of electrodes

for measurement of nerve conduction velocity of neuronal extensions with induced myelin in a 3D structure. The versatility of the model and its capability to successfully form myelin in 3D through either the inclusion of exogenous SC or the induced migration of endogenous SC makes this a potentially useful model system.

3.1. Presence of Myelinating Schwann Cells: Immunohistochemistry

Myelin in the peripheral nervous system is deposited by myelinating SCs. MBP is a marker that is observed preferentially in myelinating SCs. The presence of myelinating SCs was confirmed by detecting MBP utilizing fluorescence and confocal microscopy. Method A, utilizing exogenous SC made possible by the visible light photoinitiation method, showed 3D axonal growth and the presence of myelinating SCs. The MBP-stained tissue was counterstained for beta-III tubulin (B-III) to label axons, and merged images show the myelinating SCs associating with the axon tracts, a step needed before they deposit their membrane to form myelin sheaths (Figure 3A). Co-staining for B-III and MBP was also utilized to obtain confocal Z-stacks of the entire length of the tissue confirming the presence of myelinating SC in 3D throughout the constructs after 25 days in culture (Figure 3B), with a depth of MBP-positive growth of 88 ± 15 μm (Figure 3C).

Working with Method A, the effect of AA exposure duration in increasing the presence of myelinating SCs was explored with and without the addition of exogenous SCs. The control group was samples cultured in the MeDex hydrogel without the addition of exogenous SCs. Quantification of MBP staining showed that 25 days of AA exposure had significantly higher presence of myelinating SCs compared to 15 days in both the experimental and control groups, when quantified by thresholded pixel counts of MBP volume (Figure 4A). Because addition of AA also had the potentially confounding effect of increasing axonal outgrowth, likely through trophic effects from mature Schwann cells, we also quantified the presence of myelinating SCs by normalizing MBP myelin volume to the amount of axonal volume. The ratio of myelin to axonal growth was measured by quantification of MBP and B- III, and the 25-day AA exposure showed a significantly higher ratio of MBP to B-III (Figure 4B). When quantifying myelin by this method, differences among groups were more apparent. Moreover, with respect to the control group, there was significantly higher pixel counts of MBP volume and higher ratios of MBP to B-III, demonstrating that addition of the exogenous SCs greatly influences the formation of the myelin in the system.

3.2. Presence of Myelin: Histology

Light microscopy of TB-stained semithin cross-sections demonstrated the thickness of the 3D tissue formation and the high density of neurons and SCs (Figure 5A) obtained with Method A. TEM of ultrathin cross-sections of the neural tract confirmed a high density of parallel, highly-fasciculated axons, as well as the presence of SC and SC-encapsulated axons and myelin sheath formation (Figure 5 B-E). Myelin segments were consistently identified in TEM images, verifying the formation of characteristic spiral-wrapped, compact myelin (Figure 5E). These findings demonstrate that the 3D *in vitro* model enables SC to form myelin sheaths around axons. Method B, incorporating the endogenous SC preparation, also gave indication of the presence of myelin in the system through electrophysiological data (discussed in section 3.3). However, MeHp hydrogel consistently was lost during the

embedding protocol making Method B unusable for sectioning for TB-staining or to carry out TEM imaging.

3.3. Effect of Myelin: Field Potential Recording

Myelin is known to act as an insulator and increase the speed of action potential propagation by promoting saltatory conduction along the axon. Thus, the physiological effect of myelination in the 3D tissue constructs was investigated by the evaluation of CAP amplitude and NCV using extracellular field potential recording. Utilizing Method B, consisting of endogenous SC in MeHp hydrogel, Schwann cell migration and neurite outgrowth from DRG explants was promoted for 10 days in a premyelination medium. Field recordings were measured after 2, 3, and 4 weeks of exposure to myelination media containing AA and compared to the same medium without AA. Results showed that longer exposure to myelination medium containing AA led to significantly higher NCV at 2, 3, and 4 weeks, and significantly greater CAP amplitude at 3 and 4 weeks (Figure 6).

Due to the transparent nature of the MeHp hydrogel – crosslinked with I2959 and UV light – field recordings were easily obtained through manual placement of electrodes. However, this hydrogel curing approach precluded field recordings of constructs with exogeneous SC, as these cells did not tolerate UV irradiation during the crosslinking process (data not shown). In contrast, SC were able to survive photo-encapsulation during the visible light-initiated MeDex system, where riboflavin was utilized as the photoinitiator[37]. But riboflavin's natural pigmentation resulted in a partially opaque hydrogel. This resulted in difficulty observing axons grown within the channel under a stereo microscope with a light source, which created difficulty for optimal placement of electrodes.

4. Discussion

The present study describes a 3D system comprising SC and neurons, which provides a useful model of the native PNS with its complex myelin architecture. This study presents two parallel models of neurite growth and myelination by the interaction of neurons and SC in order to provide a strong biomimetic tool to study the PNS and myelination phenomena. To achieve these models, we utilized a 3D polymer network and micropatterning system that was previously designed to enable spatiotemporal control of the placement of axon guidance molecules as well as the alteration of physical properties[28–33]. In this study, the micropatterned hydrogel platform was adapted for the development of a 3D culture model of peripheral myelin that accommodated two separate approaches. The first approach used a visible light cured MeDex hydrogel with the addition of exogenous SC, while the second approach used a UV cured MeHp hydrogel utilizing endogenous SC. The MeDex samples enabled histological processing of the tissue for antibody staining and TEM imaging to confirm presence of axons and myelin. MeHp samples were optically clear enabling easy electrode placement during electrophysiological studies to obtain metrics such as conduction velocity and amplitude, analogous to gold standard clinical measurements.

Both approaches used explanted DRGs as the source of PNS nerve tissue. Two cell culture media treatments were used for myelination induction (Table 1). The premyelination media contained factors that have been well-characterized and are known to support DRG and SC

growth[36,37], though it is not specialized for myelin formation. The myelination media contained FBS in conjunction with AA which stimulates myelination in 2D cultures. Specifically, researchers have found that AA may promote SC in co-culture with DRGs to generate myelin by enabling them to form a complete extracellular matrix with basal lamina[38–42]. In addition, laminin, which has been shown to be necessary for myelin formation, was incorporated into both hydrogel matrices in all experimental groups[26,43].

The key strengths of this model system include its flexibility in manipulating the microenvironment and its ability to quantify myelin formation using physiological-relevant metrics. In the preparation incorporating exogenous SC in MeDex (Method A), myelin formation was confirmed using immunofluorescent staining and confocal imaging, and TEM. Fluorescent images showed the presence of myelinating SCs associating themselves with the axon tracts. TEM images further confirm the existence of myelin sheaths around the axons. In the preparation utilizing endogenous SC in MeHp (Method B), the presence of myelin was identified in the system using the field potential electrophysiological testing with the same basic principles from our previous work[25]. Samples exposed to myelination media containing AA, a key factor which triggers SC myelination, exhibited faster NCV with respect to samples that were exposed to media without AA as shown in Figure 6. The myelinated tissue also had a higher CAP amplitude which could be attributed to a higher degree of fiber fasciculation leading to a greater population of stimulated fibers. In addition, increased exposure time to myelination media with AA resulted in higher CAP and NCV values as shown in Figure 6. This confirms the importance of the role of AA in the formation, deposition, and maintenance of myelin.

While the uniqueness of this model system provides certain advantages, it is not without its limitations. While each version of the model was able to overcome significant challenges, such as the low tolerance of SC to UV light and incompatibility of the MeHp gel with histology processing, the need for separate models does prevent certain observations or comparisons that could be useful. For example, noting the effects of adding exogenous SC on both conduction velocity and myelin sheath formation would be instructive, as would being able to correlate structural variations with functional outcomes. These comparisons would not be possible in this system as currently conceived. Also, in contrast to conventional cell cultures, the use of intact tissue explants may lead to increased sample-to-sample variability due to the skill of the dissector and unavoidable variations in explant quality and cell number. Further, while measuring nerve conduction and histology in vitro can be advantageous, these metrics may not be appropriate for applications such as drug discovery, which requires a high-throughput assay.

In combination, the two parallel approaches described were able to meet the objective of creating a 3D myelinated PNS nerve culture from which histological or electrophysiological studies could be done. This novel platform will be useful for studies of peripheral myelin disorders and for screening experimental drugs for safety and/or efficacy. Future work will focus on a developing a system that allows for both histological and electrophysiological testing within the same construct for use in myelination studies and neurotoxic drug screening. Furthermore, this model can be easily expanded to integrate other cell types in a unique 3D *in vitro* model in order to investigate other neurological phenomena.

5. Conclusion

This work reports the development of a novel *in vitro* 3D co-culture biomimetic hydrogel model of a myelinated peripheral nerve. By utilizing a facile high-throughput photolithography method, we were able to engineer two unique 3D microenvironments to replicate neuronal phenomena by co-culturing DRG explants and SC. Exogenous SC cultured in a MeDex hydrogel allowed for visualization of myelin existence and structure, while the migration of endogenous SC cultured in a MeHp hydrogel enabled electrophysiological measurements of NCV that confirmed myelin presence. Furthermore, culture media regimens supplemented with ascorbic acid were found to improve the quantity of myelination found within the system. Taken together, these two complementary models provide the basis for development of a myelinated peripheral nerve-on-a-chip model that enables the collection of clinically relevant endpoints for potential drug screening applications.

Acknowledgements

The authors thank Mr. Reed Gioe for assistance with MatLab scripting and Ms. Devon Bowser for help editing the manuscript. Portions of this work were supported by the DOD (W82XWH-12–1-0246) and the NIH (R41-TR001270).

References

1. Skardal A, Shupe T & Atala A Organoid-on-a-chip and body-on-a-chip systems for drug screening and disease modeling. Drug Discov. Today 21, 1399–1411 (2016). [PubMed: 27422270]
2. Zhang B & Radisic M Organ-on-a-chip devices advance to market. Lab Chip 17, 2395–2420 (2017). [PubMed: 28617487]
3. Kola I & Landis J Can the pharmaceutical industry reduce attrition rates? Nat. Rev. Drug Discov 3, 1–5 (2004).
4. Haring AP, Sontheimer H & Johnson BN Microphysiological Human Brain and Neural Systems-on-a-Chip: Potential Alternatives to Small Animal Models and Emerging Platforms for Drug Discovery and Personalized Medicine. Stem Cell Rev. Reports 13, 381–406 (2017).
5. Yi Y, Park J, Lim J, Lee CJ & Lee SH Central Nervous System and its Disease Models on a Chip. Trends Biotechnol. 33, 762–776 (2015). [PubMed: 26497426]
6. Manji H Drug-induced neuropathies Handbook of Clinical Neurology 115, (Elsevier B.V., 2013).
7. Astashkina A & Grainger DW Critical analysis of 3-D organoid in vitro cell culture models for high-throughput drug candidate toxicity assessments. Adv. Drug Deliv. Rev 69–70, 1–18 (2014).
8. Lelievre SA, Kwok T & Chittiboyina S Architecture in 3D cell culture: An essential feature for in vitro toxicology. Toxicol. Vitr 0–1 (2016). doi:10.1016/j.tiv.2017.03.012
9. Boerboom A, Dion V, Chariot A & Franzen R Molecular Mechanisms Involved in Schwann Cell Plasticity. Front. Mol. Neurosci 10, (2017).
10. Sherman DL & Brophy PJ Mechanisms of axon ensheathment and myelin growth. Nat. Rev. Neurosci 6, 683–90 (2005). [PubMed: 16136172]
11. Tzvetanova ID & Nave K-A Axons hooked to Schwann cell metabolism. Nat Neurosci 17, 1293–1295 (2014). [PubMed: 25254976]
12. Hyung S et al. Coculture of Primary Motor Neurons and Schwann Cells as a Model for In Vitro Myelination. Sci. Rep 5, 15122 (2015). [PubMed: 26456300]
13. Desai A, Kisaalita WS, Keith C & Wu ZZ Human neuroblastoma (SHSY5Y) cell culture and differentiation in 3-D collagen hydrogels for cell-based biosensing. Biosens. Bioelectron 21, 1483–1492 (2006). [PubMed: 16084714]

14. Irons HR et al. Three-dimensional neural constructs: a novel platform for neurophysiological investigation. J. Neural Eng 5, 333–341 (2008). [PubMed: 18756031]
15. Lai Y, Cheng K & Kisaalita W Three Dimensional Neuronal Cell Cultures More Accurately Model Voltage Gated Calcium Channel Functionality in Freshly Dissected Nerve Tissue. PLoS One 7, (2012).
16. Frega M, Tedesco M, Massobrio P, Pesce M & Martinoia S Network dynamics of 3D engineered neuronal cultures: a new experimental model for invitro electrophysiology. Sci. Rep 4, 5489 (2014). [PubMed: 24976386]
17. Ulloa Severino FP et al. The role of dimensionality in neuronal network dynamics. Sci. Rep 6, 29640 (2016). [PubMed: 27404281]
18. Crone C & Krarup C Neurophysiological approach to disorders of peripheral nerve. Handb. Clin. Neurol 115, 81–114 (2013). [PubMed: 23931776]
19. Arezzo JC, Litwak MS & Zotova EG Correlation and Dissociation of Electrophysiology and Histopathology in the Assessment of Toxic Neuropathy. Toxicol. Pathol 39, 46–51 (2011). [PubMed: 21119050]
20. Carriel V, Garzón I, Alaminos M & Cornelissen M Histological assessment in peripheral nerve tissue engineering. Neural Regen. Res (2014). doi:10.4103/1673-5374.141798
21. Halpern JS Lower extremity peripheral nerve assessment. J. Emerg. Nurs 15, 333–337 (1989). [PubMed: 2668599]
22. Valdivia P et al. Multi-well microelectrode array recordings detect neuroactivity of ToxCast compounds. Neurotoxicology 44, 204–217 (2014). [PubMed: 24997244]
23. Johnstone AFM et al. Microelectrode arrays: A physiologically based neurotoxicity testing platform for the 21st century. NeuroToxicology 31, 331–350 (2010). [PubMed: 20399226]
24. Radio NM & Mundy WR Developmental neurotoxicity testing in vitro: Models for assessing chemical effects on neurite outgrowth. NeuroToxicology 29, 361–376 (2008). [PubMed: 18403021]
25. Huval RM et al. Microengineered Peripheral Nerve-on-a-Chip for Preclinical Physiological Testing. Lab Chip 15, 2221–2232 (2015). [PubMed: 25850799]
26. Curley JL & Moore MJ Facile micropatterning of dual hydrogel systems for 3D models of neurite outgrowth. J. Biomed. Mater. Res. A 99, 532–43 (2011). [PubMed: 21936043]
27. Khoshakhlagh P, Bowser DA, Brown JQ, Moore MJ. Comparison of visible and UVA phototoxicity in neural culture systems micropatterned with digital projection lithography. J Biomed Mater Res A, accepted.
28. Horn-Ranney EL, Curley JL, Catig GC, Huval RM & Moore MJ Structural and molecular micropatterning of dual hydrogel constructs for neural growth models using photochemical strategies. Biomed. Microdevices 15, 49–61 (2013). [PubMed: 22903647]
29. Curley JL, Jennings SR & Moore MJ Fabrication of Micropatterned Hydrogels for Neural Culture Systems using Dynamic Mask Projection Photolithography. J. Vis. Exp 1–6 (2011). doi: 10.3791/2636
30. Catig GC, Figueroa S & Moore MJ Experimental and computational models of neurite extension at a choice point in response to controlled diffusive gradients. J. Neural Eng 12, (2015).
31. Lowry Curley J, Catig GC, Horn-Ranney EL & Moore MJ Sensory Axon Guidance with Semaphorin 6A and Nerve Growth Factor in a Biomimetic Choice Point Model. Biofabrication 6, (2014).
32. Horn-Ranney EL, Khoshakhlagh P, Kaiga JW & Moore MJ Light-reactive dextran gels with immobilized guidance cues for directed neurite growth in 3D models. Biomater. Sci 2, 1450 (2014).
33. Khoshakhlagh P & Moore MJ Photoreactive interpenetrating network of hyaluronic acid and Puramatrix as a selectively tunable scaffold for neurite growth. Acta Biomater. 16, 23–34 (2015). [PubMed: 25617804]
34. Zhou S, Bismarck A & Steinkeb JHG Interconnected macroporous glycidyl methacrylate-grafted dextran hydrogels synthesised from hydroxyapatite nanoparticle stabilised high internal phase emulsion templates. J. Mater. Chem 22, 18824–18829 (2012).

35. Dijk-Wolthuis WNE van et al. Synthesis, Characterization, and Polymerization of Glycidyl Methacrylate Derivatized Dextran. Macromolecules 28, 6317–6322 (1995).

36. Eshed Y et al. Gliomedin mediates Schwann cell-axon interaction and the molecular assembly of the nodes of Ranvier. Neuron 47, 215–229 (2005). [PubMed: 16039564]

37. Kim S & Chu C Visible Light Induced Dextran-methacrylate Hydrogel Formation Using (−)-Riboflavin Vitamin B2 as a Photoinitiator and L-arginine as a Co-initiator. Fibers Polym. 10, 14–20 (2009).

38. Zuchero JB & Barres BA Between the Sheets: A Molecular Sieve Makes Myelin Membranes. Dev. Cell 21, (2011).

39. Bunge MB, Williams ANNK, Wood PM & Jeffrey JJ COMPARISON OF NERVE CELL AND NERVE CELL PLUS SCHWANN CELL CULTURES, WITH PARTICULAR EMPHASIS ON BASAL LAMINA AND COLLAGEN FORMATION The availability of cultures of normal nerve cells (NCs) and Schwann cells (SCs) with and without fibroblasts has allo. 84, (1980).

40. Eldridge CF, Bunge MB, Bunge RP & Wood PM Differentiation of axon-related Schwann cells in vitro. I. Ascorbic acid regulates basal lamina assembly and myelin formation. J. Cell Biol 105, 1023–1034 (1987). [PubMed: 3624305]

41. Bottenstein JE & Sato GH Growth of a rat neuroblastoma cell line in serumfree supplemented medium (growth regulation/B104 cells/neurite extension/central nervous system). Neurobiology 76, 514–517 (1979).

42. Podratz JL, Rodriguez EH & Windebank AJ Antioxidants Are Necessary for Myelination of Dorsal Root Ganglion Neurons, In Vitro. *Glia* 45, 54–58 (2004). [PubMed: 14648545]

43. Chernousov MA, Yu W-M, Chen Z-L, Carey DJ & Strickland S Regulation of Schwann cell function by the extracellular matrix. Glia 56, 1498–1507 (2008). [PubMed: 18803319]

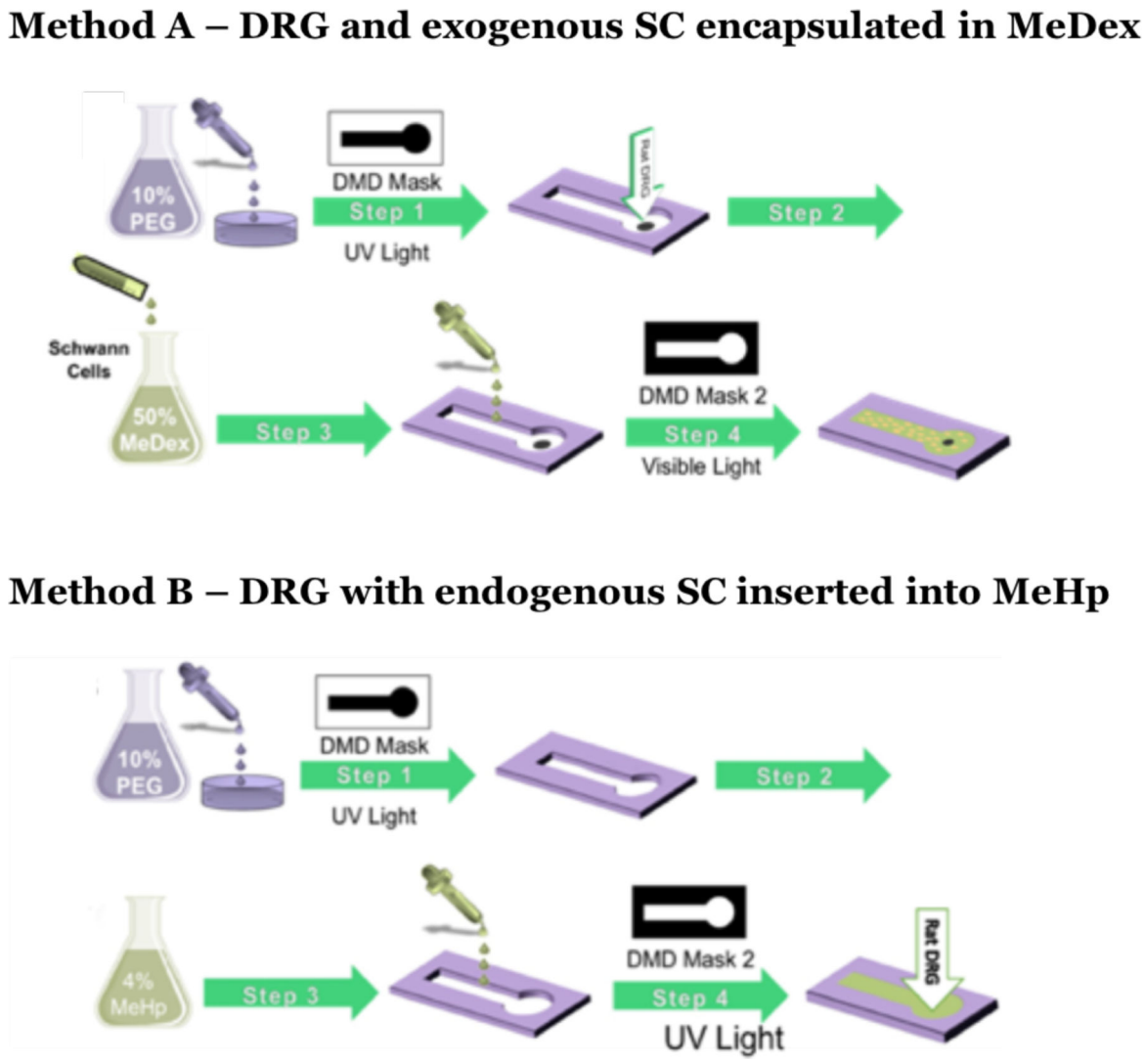

Figure 1.

Depiction of the methodology for co-culturing SC and DRGs. For Method A, utilizing exogenous SC in MeDex, Step 1: Formation of PEG mold; Step 2: DRG insertion; Step 3: Mixing SC with the gel solution at a specific cell count and addition of the gel solution to the void; Step 4: Irradiation using the negative mask and gel formation. For Method B, utilizing endogenous SC MeHp, Step 1: Formation of PEG mold; Step 2: Filling up the void with gel solution; Step 3: Irradiation using the negative mask and gel formation; Step 4: DRG insertion.

Figure 2.
Sample construct with placement of recording (left) and stimulating (right) electrodes placed within DRG and dense neural growth tract in channel, respectively, for field recording.

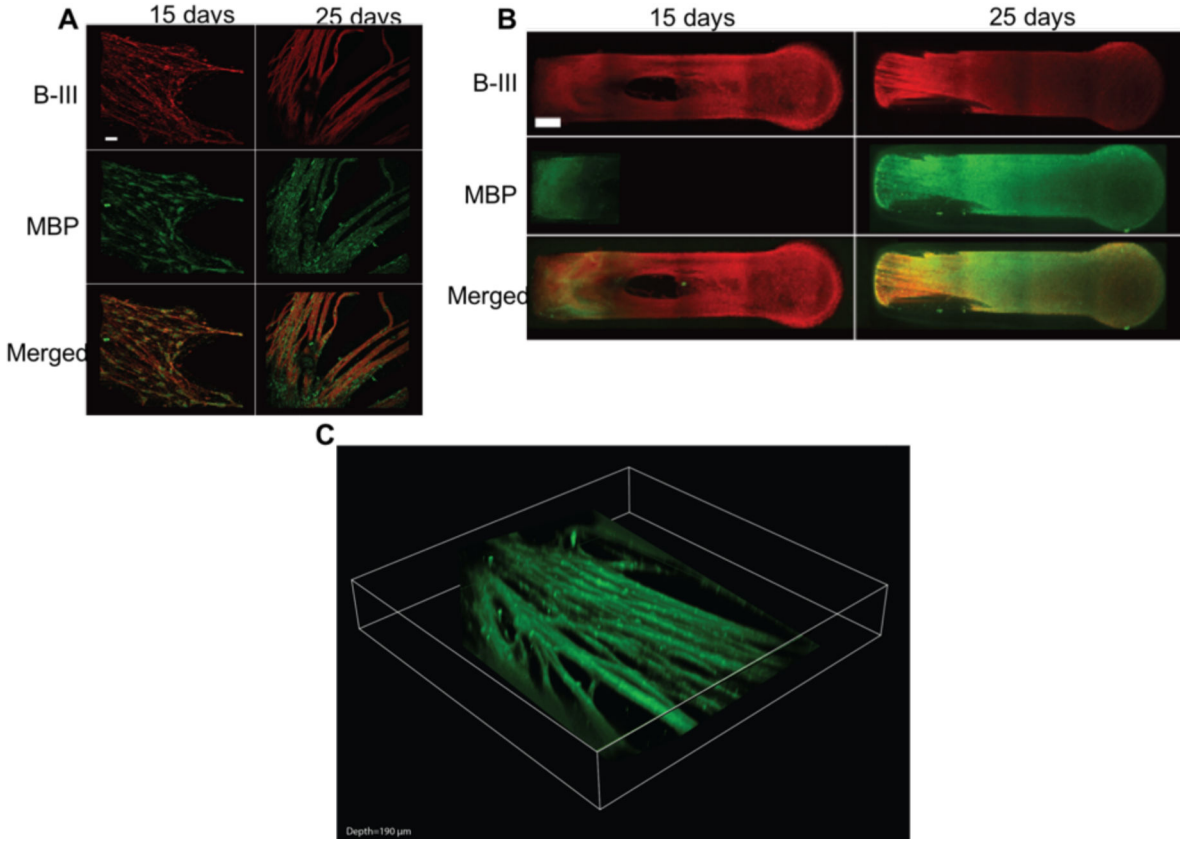

Figure 3.

Antibody staining results of DRG cultured in a MeDex hydrogel utilizing exogenous SCs A) Development of MBP after 25 days. DRG/SC co-cultured with neurons fixed and immunolabeled with anti-MBP and B-III antibodies for myelinating SCs and axons. Objective 20X; Scale bar = 25 μm. SC completely envelop axons after 25 days, forming MBP-positive axons in all experimental groups. B) The immunohistochemistry shows axons (B-III, red) and myelin basic protein, (MBP, green). The figures are acquired using Z-stack acquisition with confocal microscopy. A maximum intensity projection shows dense fasciculated growth after 25 days. Scale bar = 500 μm. C) 3D volume view Z-stack rendering (MBP, green 190 µm volume of scan thickness)

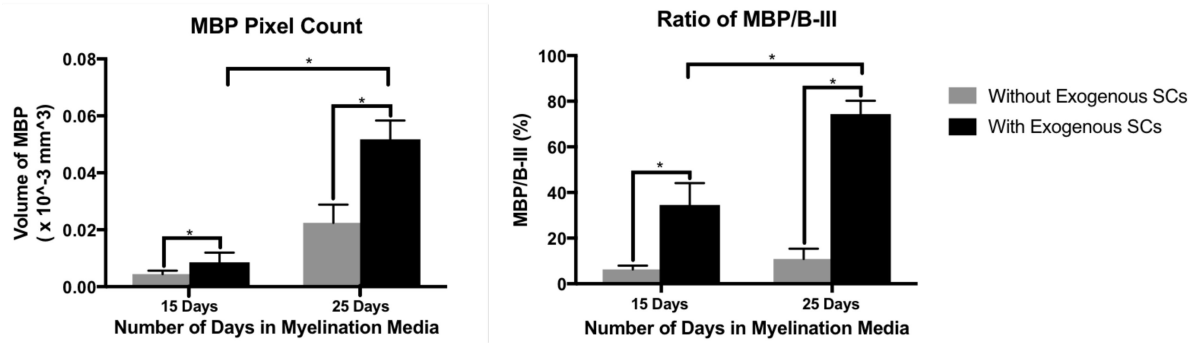

Figure 4.

Volume and myelin quantification of samples grown in MeDex hydrogel utilizing exogenous SCs A) Volume of MBP is shown. The amount of MBP (in terms of pixel count) increased significantly with longer exposure to AA, and with addition of exogenous SCs. B) The ratio of the volume of MBP to the volume of B-III tubulin more clearly demonstrates the effects of longer exposure to AA and addition of endogenous cells to induce the formation of SCs from the proliferative to the myelinating phenotype. ($n = 3–5$, $p < 0.05$)

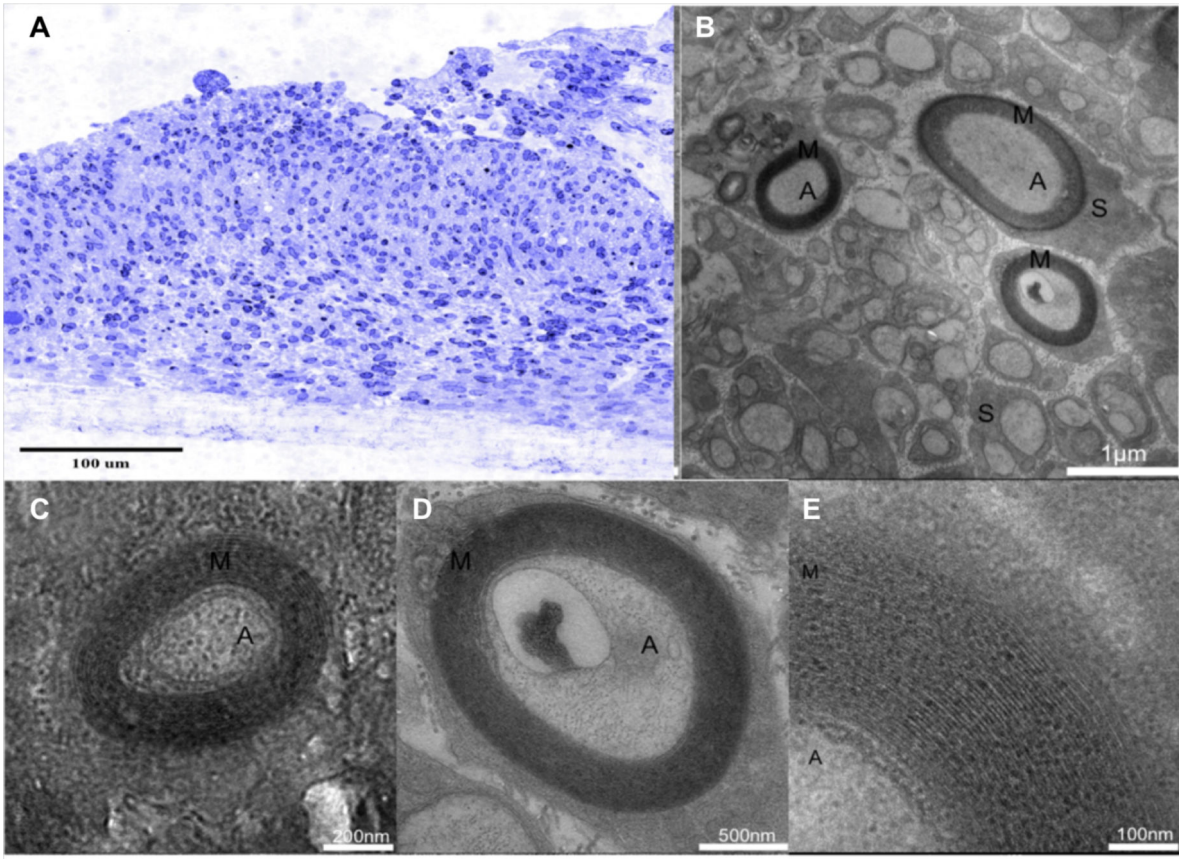

Figure 5.

Histological results of samples cultured in MeDex hydrogel A) Semithin cross-section stained with TB. TEM of neural culture cross-sections demonstrate myelin sheaths around individual nerve fibers in 15 and 25-day cultures. B) High density of parallel, neurite fascicles in the construct. C) 25 days in myelination media. D) 15 days in myelination media. E) Layered myelin sheath around the axon. A: Axons, M: Myelin, S: Schwann cells.

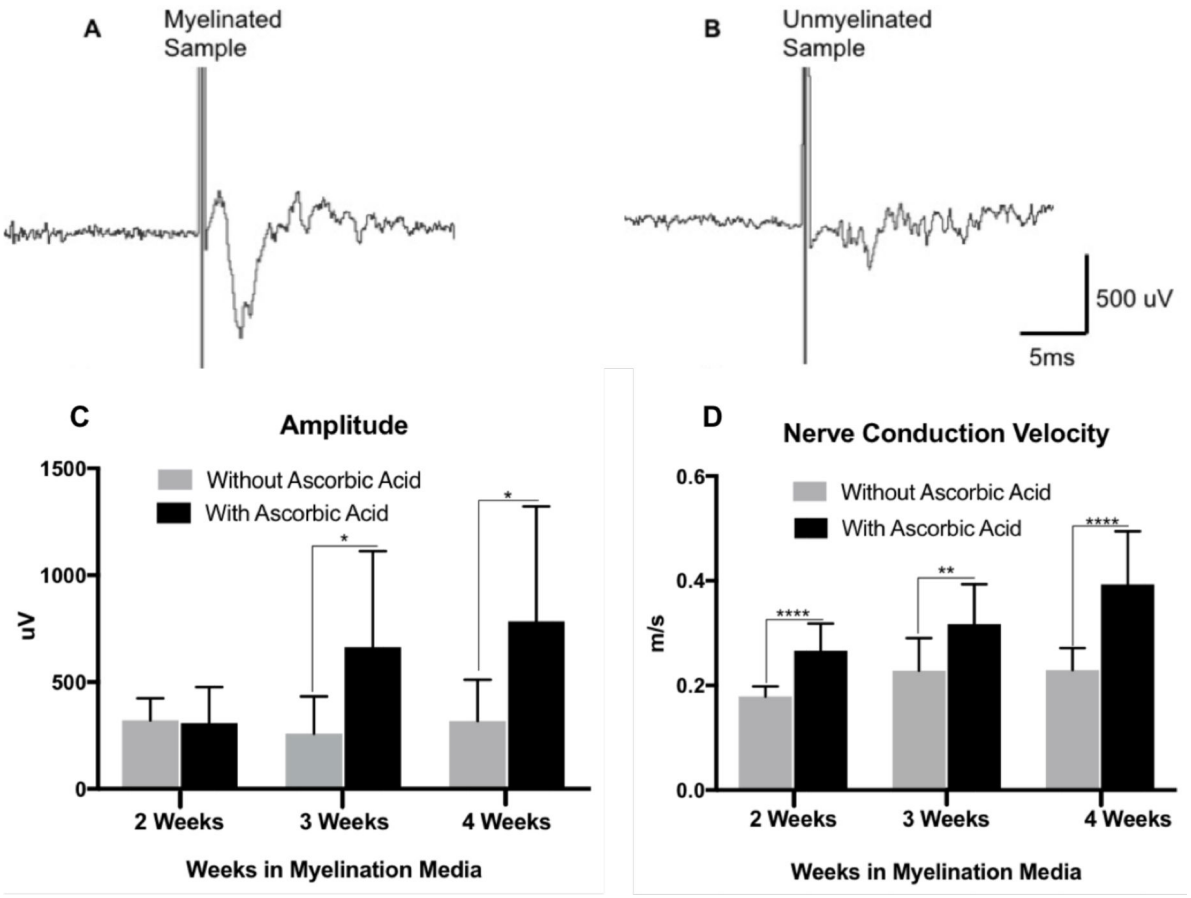

Figure 6.

Example trace of population responses demonstrating successful field potential recordings in 3D neural constructs and waveform properties characteristic of a CAP and NCV. Samples were cultured according to Method B utilizing endogenous SC in MeHp hydrogel. A) Sample trace of 4-week myelinated construct exposed to AA. B) Sample trace of 4-week myelinated construct not exposed to AA. C) CAP comparison between constructs not exposed to AA and constructs exposed to AA. Higher CAP is observed in constructs exposed to AA and increased CAP is observed with longer exposure to myelination media containing AA past 3 weeks D) NCV comparison between constructs not exposed to AA and constructs exposed to AA. Higher NCV is observed in constructs exposed to AA and increased NCV is observed with longer exposure to myelination media containing AA. (n = 12; *p < 0.05; **p < 0.01; ***p < 0.001)

Table 1.

Components of myelination inducing media regimen

Myelination Media Regimen	Neural Growth Media	Premyelination Media	Myelination Media
Neurobasal Media	X		
Basal Medium Eagle		X	X
NGF	X	X	X
B-27 Supplement	X		
ITS Supplement		X	X
D-Glucose		X	X
BSA		X	
AA			X
Anti-Anti	X	X	X
Glutamax	X	X	X
FBS			X